The Journal of Immunology

Clonal Selection, Clonal Senescence, and Clonal Succession: The Evolution of the T Cell Response to Infection with a Persistent Virus

Miles P. Davenport, Chrysoula Fazou, Andrew J. McMichael and Margaret F. C. Callan

J Immunol 2002; 168:3309-3317; ;
doi: 10.4049/jimmunol.168.7.3309
http://www.jimmunol.org/content/168/7/3309

The Journal of Immunology is published twice each month by
The American Association of Immunologists, Inc.,
1451 Rockville Pike, Suite 650, Rockville, MD 20852

Print ISSN: 0022-1767 Online ISSN: 1550-6606.

Clonal Selection, Clonal Senescence, and Clonal Succession: The Evolution of the T Cell Response to Infection with a Persistent Virus[1]

Miles P. Davenport,* Chrysoula Fazou,† Andrew J. McMichael,‡ and Margaret F. C. Callan[2‡]

We have analyzed the CD8$^+$ T cell response to EBV and find that a larger primary burst size is associated with proportionally greater decay during the development of memory. Consequently, immunodominance and clonal dominance are less marked in memory than primary responses. An intuitive interpretation of this finding is that there is a limit to the number of cell divisions a T cell clone can undergo, and that the progeny of clones that have expanded massively during a primary immune response are more prone to die as a result of senescence. To test this hypothesis, we have derived a mathematical model of the response of different T cell clones of varying avidity for Ag in the primary and persistent phases of viral infection. When cellular survival and replication are linked to T cell avidity for Ag and Ag dose, then high-avidity T cells dominate both the primary and secondary responses. We then incorporated a limit in the number of cell divisions of individual T cell clones to test whether such a constraint could reproduce the observed association between cell division number and alterations in the contribution of clones to the response to persistent infection. Comparison of the model output with the experimental results obtained from primary and persistent EBV infection suggests that there is indeed a role for cellular senescence in shaping the immune response to persistent infection. ***The Journal of Immunology*****, 2002, 168: 3309–3317.**

The CD8$^+$ T cell population plays an important role in controlling both primary and persistent/secondary virus infection. Extensive analysis of the evolution of T cell responses in mouse models of infection has been undertaken (1–8). The emerging picture is that during the primary response, there is both selection of dominant epitopes and epitope-driven selection of dominant T cell clones. The emergence of the memory pool of T cells during the down-regulation of the primary response is predominantly a stochastic process and does not appear to be characterized by further selection. Subsequent restimulation of the memory pool may, however, be characterized by further epitope-driven clonal selection of T cells and increased narrowing of the response.

Analysis of the evolution of CD8$^+$ T cell responses in humans has relied on studies of natural infection. Our work has focused on the response to EBV and has involved an analysis of the Ag specificity and clonal composition of the CD8$^+$ T cell response to the virus during the primary phase of infection (the primary response) and 1 year later, during the persistent phase of infection with the virus (the memory response; in the context of EBV infection, we use this term to describe the response that persists following resolution of primary infection). The results uphold the concepts that epitope selection and clonal dominance may be a feature of primary responses (9, 10) and that the primary clonal burst is followed by decay in the response (9, 11). However, comparison of the epitope specificity and clonal composition of the CD8$^+$ T cell response to EBV during the primary and memory responses reveals surprising changes in the hierarchies of dominance both at the level of the epitope and, in some responses, at the level of the T cell clones responding to these epitopes (12). At the level of the epitope, we find that the most dominant responses are most extensively down-regulated during the resolution of the primary response and these responses actually become relatively less dominant in memory (12, 13). At the level of the T cell clones responding to the epitopes, we also find that, in many instances, the clones that dominate the primary response to an epitope are most heavily down-regulated, leaving other clones to dominate the memory response. Thus, ongoing focusing of the response to EBV does not occur. In this study, we report an analysis of the data and show that the extent of down-regulation of the responses is related to the logarithm of the number of cells that mediate the primary response. We suggest an explanation for the findings based on the assumption that individual T cell clones do not have an infinite life span and that clonal survival may diminish with increasing turnover (14). We propose that, if a T cell clone has divided extensively during the primary immune response, many of the progeny will die, leaving relatively few cells to contribute to the memory response (12). To test this hypothesis, we developed models of T cell replication and death (see Fig. 1). The first, basic model is adapted from mathematical models that have been used previously to analyze CD8$^+$ T cell responses to virus infection (15, 16). Thus, we explicitly incorporate 1) variation in avidity of different responding T cell clones and 2) a dependence of cell division rate on the avidity of the cell for Ag and on the abundance of Ag. We compare this basic model with a second model that includes 1) an explicit accounting for cell division number and 2) a decline in survival with increased cell division number. We apply these models to our previously published data and to some new data and find

*Theoretical Biology and Biophysics, Los Alamos National Laboratory, Los Alamos, NM 87545; †University of New South Wales, Kensington, New South Wales, Australia; and ‡Institute of Molecular Medicine, John Radcliffe Hospital, Oxford, United Kingdom

Received for publication September 28, 2001. Accepted for publication February 1, 2002.

The costs of publication of this article were defrayed in part by the payment of page charges. This article must therefore be hereby marked *advertisement* in accordance with 18 U.S.C. Section 1734 solely to indicate this fact.

[1] This work was supported by a grant from the Medical Research Council of the United Kingdom.

[2] Address correspondence and reprint requests to Dr. Margaret F. C. Callan, Institute of Molecular Medicine, John Radcliffe Hospital, Oxford, OX4 1DQ, U.K. E-mail address: mcallan@molbiol.ox.ac.uk

0022-1767/02/$02.00

that it is the outcome of the second model that most closely resembles the observed relationship between the primary and memory responses to this virus. This result strongly implies that T cell senescence is an important process that prevents excessive immune focusing over time, and hence helps to mold optimal memory T cell responses.

Materials and Methods

Patients and samples

Six patients positive for the *HLA-A2* allele, four patients positive for the *HLA-B8* allele, and one patient positive for both alleles were identified during the acute stage of infectious mononucleosis due to primary EBV infection. Samples of peripheral blood were taken from the patients immediately after diagnosis. In general, patients had had symptoms for a period of 1–3 wk before the diagnosis was made. Further samples of peripheral blood were taken 1 year later, at which time all the patients had made a complete clinical recovery from infectious mononucleosis. PBMC were separated using Lymphoprep (Axis-Shield, Oslo, Norway) density gradient centrifugation.

Staining of PBLs with HLA-peptide tetrameric complexes

Soluble PE-labeled HLA-peptide tetrameric complexes were produced as previously described (9). For the purposes of this study, we constructed tetramers of HLA-A2 complexed with the GLCTLVAML epitope from the EBV lytic protein BMLF1 (17), of HLA-B8 complexed with the RAKFKQLL epitope from the EBV lytic protein BZLF1 (18), and of HLA-B8 complexed with the FLRGRAYGL epitope from the EBV latent protein EBV-encoded nuclear Ag 3A (19). PBMC were incubated with 5 μl tetramer in solution at a concentration of 1 μmol/L on ice for 30 min. The cells were washed and stained with a tricolor-conjugated anti-CD8 mAb (Caltag Laboratories, Burlingame, CA) and were analyzed on a FACSCalibur using CellQuest software (BD Biosciences, Oxford, U.K.).

Analysis of TCR V chain usage by T cells specific for EBV epitopes

Samples of PBMC were stained with one of a panel of mAbs specific for the human TCR V chains, washed, and then stained with a FITC-conjugated anti-mouse or anti-rat mAb (DAKO, Carpinteria, CA). Following this, the cells were washed, stained sequentially with the relevant HLA-peptide tetrameric complex and anti-CD8 mAb, and analyzed, as above. The Vβ2 mAb was found to interfere with the binding of the HLA-A2/GLCTLVAML tetramer in some patients, and therefore results obtained using this mAb were omitted from the analysis of GLCTLVAML-specific T cells.

Estimation of the avidity and dissociation kinetics of the interaction between the HLA-B8/RAKFKQLL tetramer and the RAKFKQLL-specific CD8$^+$ T cells

Samples of PBMC from blood taken during the primary and persistent phases of EBV infection were stained with saturating concentrations of PE-labeled HLA-B8/RAKFKQLL tetramer at 4°C. The PBMC were washed, and an aliquot of cells was removed for FACS analysis. The remaining PBMC were incubated with a 100-fold excess of unlabeled HLA-B8/RAKFKQLL tetramer at 4°C. This unlabeled reagent effectively blocked binding/rebinding of PE-labeled tetramer. Further aliquots of cells were removed and analyzed by FACS at seven time points. The total fluorescence within the PE-positive gate was plotted against time to give the dissociation curve. This total fluorescence was calculated as the sum of the fluorescence intensities of the tetramer-positive cells normalized per lymphocyte. This was then normalized to percentage of the total fluorescence at the initial time point and plotted on a logarithmic scale. An initial experiment was performed using an HLA-B8-restricted RAKFKQLL-specific T cell clone. Results confirmed that the plot of the logarithm of normalized fluorescence against time was linear and revealed that the $t_{1/2}$ of dissociation was 46.8 min at 4°C.

To estimate apparent K_d values for the interaction between RAK FKQLL-specific T cells and the HLA-B8/RAKFKQLL tetramer, samples of PBMC were stained at room temperature with the HLA-B8/RAK FKQLL tetramer at a range of subsaturating concentrations. A graph of tetramer concentration plotted against bound tetramer (total fluorescence, calculated as above) was obtained and, in addition, Scatchard plots of bound tetramer (total fluorescence) vs bound tetramer divided by free tetramer were also drawn. The absolute values for total fluorescence were larger for PBMC from primary infection because of the higher frequency of Ag-specific T cells in these samples. This, however, does not affect the calculation of the apparent K_d. The tetramer was in vast excess, and therefore the concentration of free tetramer was taken as being equal to the concentration of the tetramer in the staining solution. The apparent K_d was derived by the nonlinear fitting method from the graph of tetramer concentration plotted against bound tetramer.

Mathematical modeling of the T cell response

The basic model of the T cell response to EBV is shown in Fig. 1*a* and was adapted from published mathematical models of the CD8$^+$ T cell response to virus infection in vivo (15, 16). It uses a number of ordinary differential equations to simulate the T cell response to three viral epitopes (denoted A, B, and C). The naive repertoire (N_i) recognizing each epitope consists of 10 clones that vary in their avidity for Ag (A_i). The avidity of each T cell is assigned as a randomly generated number between 0 and 10. It is assumed that T cells are stimulated by increasing doses of Ag and that, for any given level of avidity, the level of stimulation increases with increasing doses of Ag and is saturable. It is assumed that the different viral epitopes ($A-C$) are processed and presented by an infected cell with different efficiencies ($E_A - E_C$). This has the effect of producing an immunodominance hierarchy between the epitopes (17). The level of stimulation of an individual clone (S_i) is calculated by:

$$S_i = \frac{\left(\frac{YE_i}{A_i}\right)}{1 + \left(\frac{YE_i}{A_i}\right)}$$

Therefore, a clone receives 50% maximal stimulation when the total peptide presented (number of infected cells $\times$ epitopes per cell; YE) is equal to the nominal avidity of the clone. The level of stimulation of the clone is used to calculate the rate of differentiation from naive to effector cells ($S_i\omega$), the rate of proliferation of effector cells (S_iC), the rate of reactivation of memory cells ($S_i\theta$), and the rate of death of effector cells ($(1 - S_i)b_E$). Thus, increasing levels of antigenic stimulation increase the number of effector cells and decrease the death rate of effector cells. Conversely, decreasing levels of antigenic stimulation decrease the number of effector cells and increase the death rate of effector cells (12, 20–22).

Therefore, the numbers of naive effector and memory cells are described by the following differential equations:

$$\frac{dN_i}{dt} = -S_i\omega N_i$$

$$\frac{dE_i}{dt} = S_i\omega N_i + S_iCE_i + S_i\theta M_i - \phi E_i - (1 - S_i)b_E E_i$$

$$\frac{dM_i}{dt} = \phi E_i + pM_i - (S_i\theta + b_M)M_i$$

Effector cells differentiate to memory cells at a fixed rate ϕ, consistent with the observation that differentiation to memory cells appears to be stochastic and dependent on clonal burst size of the effector population (5, 8). Finally, memory cell death and division occur at a rate b_M and p, respectively. Importantly, this model allows for infinite growth of individual T cell clones.

Incorporation of a limited life span of T cell clones

To introduce the concept of replicative senescence into the model, it is necessary to keep track of the number of cell divisions that an individual T cell has undergone and then apply a maximum limit to the life span of individual T cells. The model described above was modified by the addition of different compartments of effector and memory cells that reflect the number of cell divisions the cell has undergone. The modified model is presented pictorially in Fig. 1*b*. The level of stimulation of T cells in this model is dependent on both the level of Ag and the number of cell divisions (d) the CTL have undergone. Thus, the responsiveness of T cells to Ag declines as they senesce (as d increases), such that at division cycle d_{sen} the level of antigenic stimulation for a given level of Ag has declined to half and the level of effector death is half maximal. Thus, at low antigenic stimulation, effector cells die rapidly regardless of how many cell divisions they have undergone. When antigenic stimulation is maximal, cells in early

division cycles have low death rates until they approach a high number of cell divisions (d_{sen}). The level of antigenic stimulation is calculated by:

$$S_i = \left(\frac{\left[\frac{YE_i}{A_i}\right]}{1 + \left[\frac{YE_i}{A_i}\right]} \right) \left(1 - \left\{ \frac{\left[\frac{d}{d_{sen}}\right]^3}{1 + \left[\frac{d}{d_{sen}}\right]^3} \right\} \right)$$

Mathematical modeling of viral replication

A simple mathematical model of virus replication was developed, based upon our understanding of the life cycle of EBV (Fig. 1*c*). Briefly, EBV virus infects target cells (X) to create productively infected cells (Y) that divide rapidly (at a rate "r") and produce free virus (V) at a rate "k." Productively infected cells may become latently infected (L) at a slow rate (λ). Latently infected cells may also reactivate to become productively infected at a low rate (ϵ). Productively infected cells express both lytic and latent Ags. Latently infected cells in this context refer to cells characterized by the latency I program of EBV gene expression, whereby the expression of virtually all EBV genes is down-regulated and the three Ags under consideration in this study are not expressed.

The numbers of uninfected, infected, latently infected cells, and free virus are determined by the following equations:

$$\frac{dX}{dt} = \pi - \delta X - \beta VX$$

$$\frac{dY}{dt} = \beta VX + rY + \epsilon L - (\lambda + \alpha)Y$$

$$\frac{dV}{dt} = kY - \mu V$$

$$\frac{dL}{dt} = \lambda Y - (\epsilon + \gamma)L$$

The death rates of uninfected cells (δ), latently infected cells (γ), and free virus (μ) are constant. However, the death rate of productively infected cells (α) is determined by two factors, the natural death rate of infected cells (η) and the rate of T cell killing. The overall level of cytotoxic T cell-mediated killing of the virus is determined by the total number ofeffector cytotoxic T cells. Therefore, the total death rate (α) of productively infected cells is determined by:

$$\alpha = \eta + \left[\sum_{E=A}^{E=C_i=10} \sum_{i=1} E_\chi \right]$$

That is, the natural death rate (η) plus the sum of all effector T cells from each clone (i = 1–10) specific for each epitope (A – C) times the rate of T cell killing (χ).

Results

Expansions of epitope-specific T cells in primary and persistent EBV infection

We used fluorescent-labeled HLA-peptide tetramers to analyze the frequency of $CD8^+$ T cells specific for three epitopes from EBV at two different time points (on diagnosis of primary EBV infection and 1 year later) in HLA-$A2^+$ and HLA-$B8^+$ patients. Consistent with previous studies, we found a striking $CD8^+$ T cell lymphocytosis during primary infection. Within this expanded lymphocyte population, we found populations of T cells that stained with the HLA-B8/RAKFKQLL tetramer (4.1–40% $CD8^+$ T cells) and populations of T cells that stained with the HLA-A2/GLCTLVAML tetramer (3–11% $CD8^+$ T cells). We also found small populations of $CD8^+$ T cells specific for the HLA-B8-restricted FLRGRAYGL epitope (up to 2.2% $CD8^+$ T cells) (12). The burst sizes of these primary responses are striking, suggesting that large numbers of naive T cells are recruited into the responses and/or that the cells divide multiple times during the primary response (23, 24). The initial blood samples were taken as early as possible during the primary immune response. Despite this, patients had had symptoms for 1–3 wk at the time of sampling. Work in murine models of infection suggests that the immune response may vary substantially over a short period of time during a primary infection (25). However, in two individuals we were able to analyze the T cell response at two time points, 3 wk apart, during primary infection and found that the magnitude of the responses were stable over this time period. One year later, the absolute lymphocyte counts had fallen to normal levels, but we were able to detect populations of $CD8^+$ T cells specific for the RAKFKQLL epitope (2.7–7.3% $CD8^+$ T cells), the GLCTLVAML epitope (0.5–5.5% $CD8^+$ T cells), and the FLRGRAYGL epitope (up to 1.8% $CD8^+$ T cells). In terms of absolute numbers of cells responding to a given epitope, the size of the response was always larger at the time of primary infection than it was 1 year later. Thus, the primary clonal burst was followed by a period of decay, leaving a smaller population of memory cells (24). In terms of the frequency of T cells specific for a given epitope as a proportion of the $CD8^+$ T cell population, we occasionally found that the contribution of T cells specific for a given epitope increased at 1 year. That is, the memory response was not simply a reduced version of the primary response, as has been reported in studies from other groups. Such a result would have suggested that selection of the memory pool of T cells specific for a range of epitopes was simply stochastic. We refer to this as the stochastic entry into memory hypothesis. Instead, we found that very large responses tended to decrease more than would be expected by the stochastic entry into memory model, and many smaller responses increased more than expected. We hypothesized that this may be related to senescence of the responding T cells, and therefore related to the number of cell divisions they had undergone (proportional to the logarithm of the cell number). Comparing the relationship predicted by the stochastic entry into memory hypothesis (memory = $M \times$ primary) with a relationship that allows for senescence (memory = primary $\times$ ($K - B \log_2$(primary))), we found that the latter model fitted the data better (F test, $p = 0.0056$; $R^2 = 0.43$). We then quantified the percentage of change in contribution of T cells specific for a given epitope to the $CD8^+$ T cell repertoire as follows:

$$\%\ \text{change} = \frac{(\text{proportion (1 year)} - \text{proportion (primary infection)}) \times 100}{\text{proportion (primary infection)}}$$

$$\text{where}\quad \text{proportion (1 year)} = \frac{\text{number of epitope-specific cells at 1 year}}{\text{number of CD8}^+\text{T cells at 1 year}}$$

$$\text{proportion (primary infection)} = \frac{\text{number of epitope-specific cells in primary infection}}{\text{number of CD8}^+\text{ T cells in primary infection}}$$

Contrary to the prediction of the stochastic entry into memory hypothesis that the memory response would be a fixed proportion of the primary response, we found a range from −91 to +250%, and that a higher number of cell divisions during the primary immune response is associated with a larger decrease in representation in the memory response (Fig. 2*a*).

Clonal expansions of Ag-specific T cells in primary and persistent infection

The longitudinal analysis of T cell responses to different epitopes from a persistent virus may be complicated by differences in levels of expression of different viral proteins over time. This may be particularly relevant to a comparison of responses to epitopes from latent vs lytic cycle proteins. We therefore analyzed the T cell

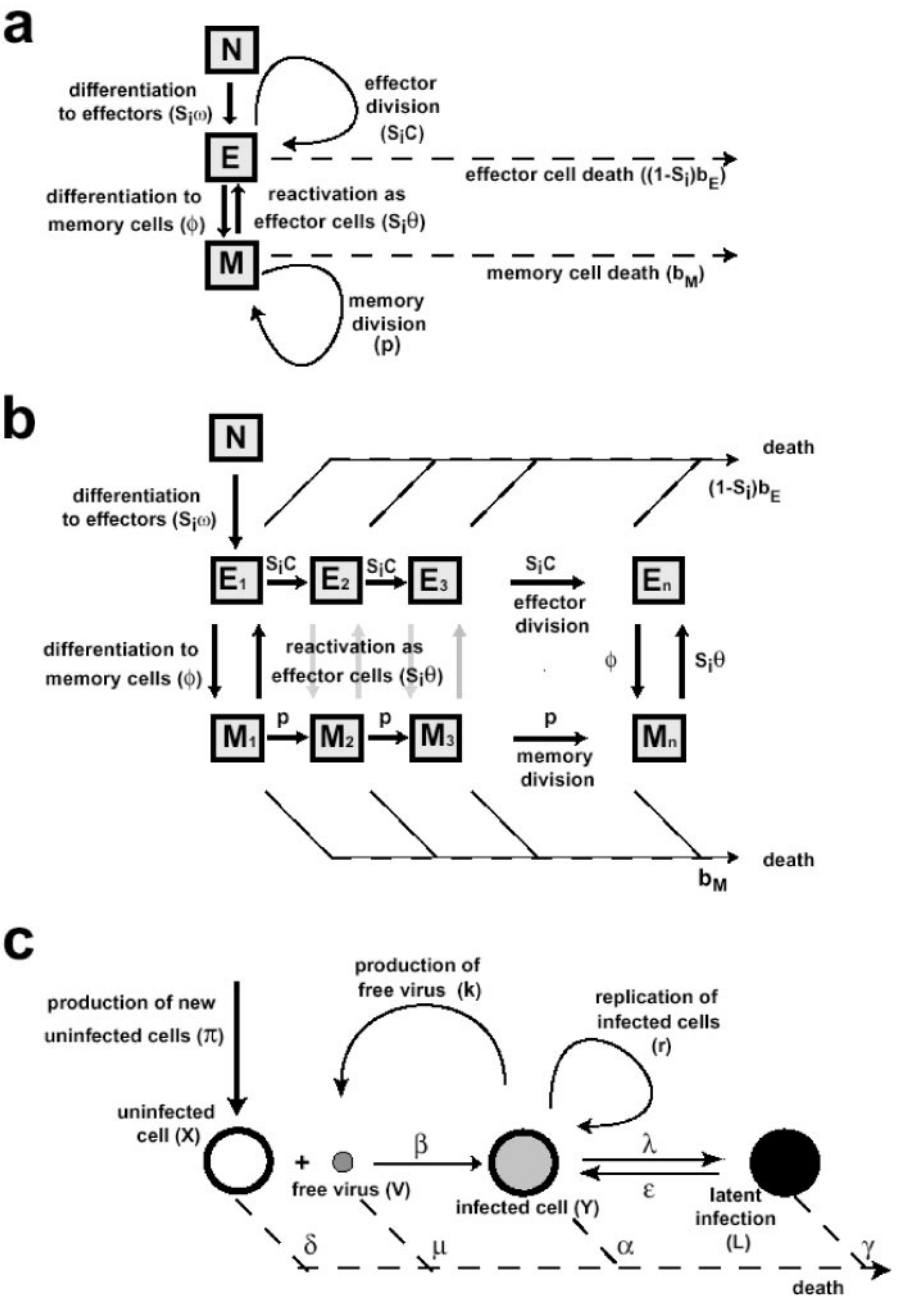

FIGURE 1. Outline of model. *a*, The basic model of T cell proliferation based on avidity for Ag and assuming no limit on cell divisions for an individual T cell clone. *b*, A model of T cell proliferation that explicitly tracks the number of divisions a T cell undergoes and incorporates cellular senescence. *c*, The dynamics of productive and latent (latency I) viral infection of target cells by EBV. Details of the model are given in *Materials and Methods*.

responses to the two lytic epitopes in more detail, focusing on the dynamics of the clones that contributed to these responses.

We combined staining with the HLA-A2/GLCTLVAML and HLA-B8/RAKFKQLL tetramers with staining using a panel of Abs specific for TCR Vβ chains and with RT-PCR to analyze the TCR use of the Ag-specific T cells. The analysis was performed on samples of peripheral blood taken as early as possible during primary infection and again on the samples taken 1 year subsequently. In two individuals, we were able to obtain samples of blood on two occasions, 3 wk apart, during primary infection. In both patients, the TCR repertoire of the Ag-specific T cells was stable over this time period. However, as previously reported, we found that the clonal and oligoclonal populations of CD8$^+$ T cells that dominated the response during primary infection were often relatively underrepresented in memory. We quantitated the percentage of change in contribution of a particular Vβ chain to an epitope-specific response from primary infection to 1 year as follows:

$$\%\ \text{change} = \frac{(\text{proportion (1 year)} - \text{proportion (primary infection)}) \times 100}{\text{proportion (primary infection)}}$$

$$\text{where}\quad \text{proportion (1 year)} = \frac{\text{number of epitope-specific cells using V}\beta\text{X at 1 year}}{\text{number of epitope-specific cells at 1 year}}$$

$$\text{proportion (primary infection)} = \frac{\text{number of epitope-specific cells using V}\beta\text{X in primary infection}}{\text{number of epitope-specific cells in primary infection}}$$

We analyzed the relationship between the percentage of change and the number of epitope-specific T cells that expressed that Vβ

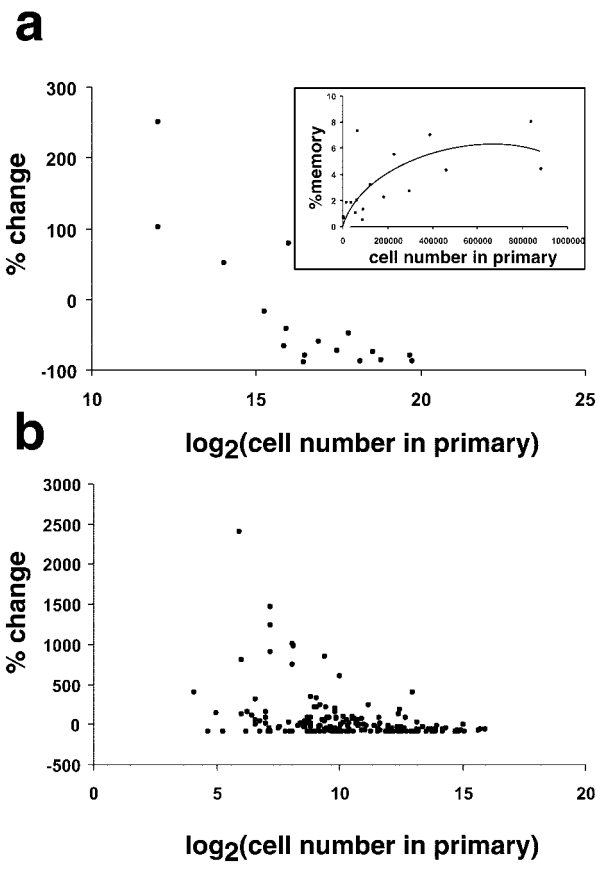

FIGURE 2. Relationship between primary response and response at 1 year. *a*, The $\log_2$ of the number of epitope-specific T cells during the primary response is plotted against the percentage of change in the frequency of T cells specific for that epitope between the primary immune response and the response at 1 year. If selection into memory was purely stochastic, then the predicted relationship would be a horizontal line. The number of epitope-specific T cells during the primary response is plotted against the percentage of these cells as a proportion of total CD8 T cells in the memory response at 1 year (*inset*). If the memory response were simply a fixed proportion of the primary response ($Y = MX$), then the relationship would be predicted to be a diagonal line. A relationship in which high cell division number in the primary response leads to a decreased contribution to the memory response ($Y = X(K - B \log_2(X))$, solid line) provides a better fit to the data ($R^2 = 0.43$; F test, $p = 0.0056$). *b*, The $\log_2$ of the number of epitope-specific T cells using a particular TCR Vβ chain is plotted against the percentage of change in frequency of epitope-specific T cells using that particular TCR Vβ chain between the primary immune response and the response at 1 year. Again, if selection into the memory pool was purely stochastic, the predicted relationship would be a horizontal line.

chain during the primary response. The relationship is more complex than that observed for the overall epitope-specific populations. The results again suggested that clones that had proliferated most extensively were less likely to contribute to memory (Fig. 2*b*). Again, if selection into the memory pool had been purely stochastic, then the relationship between percentage of change and $\log_2$ (cell number of epitope-specific cells using that Vβ in primary infection) would have been depicted by a horizontal line (the stochastic entry into memory hypothesis). Alternatively, if selection into the memory pool had been characterized by ongoing affinity maturation, there would have been a positive correlation between the parameters. Interestingly, the inverse relationship between percentage of change and $\log_2$ (cell number of epitope-specific cells using that Vβ in primary infection) did not hold true when an analysis of Vβ chains that were used by very small numbers of tetramer-reactive T cells was undertaken. These cells appeared to contribute less to the memory response than a simple semilogarithmic relationship would predict. This observation suggests that the clones that expand little during the primary response are not subject to the same constraints as those that expand most extensively. This point is discussed in further detail below.

Longitudinal analysis of the avidity and kinetics of tetramer binding to Ag-specific T cells

One explanation for a change in the TCR repertoire of Ag-specific T cells over time is that ongoing selection occurs for T cells expressing receptors with optimal kinetics of interaction with the MHC/peptide ligand (6). In two HLA-B8$^+$ individuals, we analyzed the avidity and the dissociation kinetics of the interaction between the T cells and the HLA-B8/RAKFKQLL tetramer at the two time points sampled. We found a small increase in the apparent K_d of the T cells for the tetramer (K_d = 114 nmol in primary and K_d = 134 nmol 1 year subsequently in one donor, and K_d = 110 nmol in primary and K_d = 120 nmol 1 year subsequently in the second donor) (Fig. 3, *a* and *b*, and data not shown). This small rise in K_d equates to a small fall in affinity, although it is not statistically significant at a p value of <0.05. The K_d were of a similar order of magnitude to those that have been described for the interaction between tetramers of MCC/I-Ek and the 2B4 TCR ($K_d = 60 \pm 9$ nmol) (6). The affinity of the 2B4 TCR for MCC/I-Ek has previously been estimated as 40–90 μmol at 25 degrees (26, 27). Thus, the estimates of apparent K_d we obtained are consistent with a relatively high affinity interaction, supporting the idea that, in this viral infection, selection on the basis of affinity has already occurred by the time of sampling of the primary response. Furthermore, the dissociation kinetics of the interaction between the T cells and the tetramer was also found to be very similar when T cells mediating primary vs memory responses were analyzed (Fig. 3*c* and data not shown). These results argue strongly against affinity maturation as an explanation for the observed changes in the clonal composition of the EBV-specific T cell response over time.

Modeling the T cell response to chronic viral infection

We went on to use simple mathematical models to simulate the response to infection in 20 patients. In the basic model (Fig. 1*a*), individuals differed by the random generation of avidities for each T cell clone (28). This resulted in variations in peak viremia and in dominance of individual T cell clones during the response. The data for primary infection were taken on the day of peak viral load, and those for chronic infection at day 300 in the model. This basic model produced an Ag-specific T cell repertoire in acute infection that was dominated by the highest avidity clones (Fig. 4*a*). High-avidity T cells were stimulated earlier in the response, because as the viral load gradually increased, they were sensitive to lower levels of virus. At the peak of the response, the high viral load stimulated both low and high-avidity T cells, although high-avidity T cells continued to dominate. During progression to chronic infection, low avidity clones were greatly reduced in number due to the lower viral loads. Over time, the repertoire became increasingly focused, with the high-avidity clones that dominated in acute infection coming to dominate the response to chronic infection. The picture clearly differs from that observed in the context of natural EBV infection.

We then incorporated the concept of replicative senescence into the model (Figs. 1*b* and 4*b*). Although this did not significantly alter the outcome of primary infection, it did change the predicted outcome of chronic infection. Excessive expansion during the primary response led to senescence of high-avidity T cells, resulting

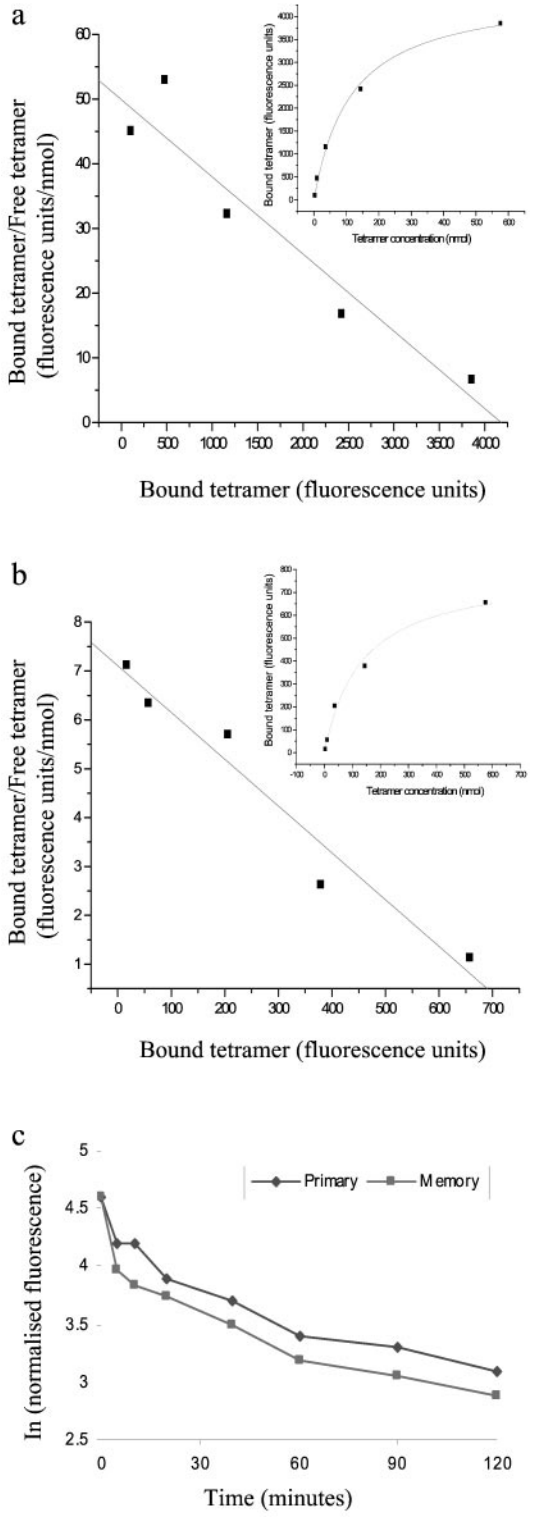

FIGURE 3. Avidity and dissociation kinetics of the interaction between the HLA-B8/RAKFKQLL tetramer and the RAKFKQLL-specific T cells during the primary immune response and 1 year later. PBMC taken from donor NS 112 during the primary (*a*) and memory (*b*) response to EBV were stained with labeled HLA-B8/RAKFKQLL tetramer at room temperature at a range of subsaturating concentrations. Plots of the concentration of tetramer against bound tetramer and Scatchard plots of bound/free tetramer vs bound tetramer were derived (*a* and *b*). In addition, the concentration of tetramer was plotted against bound tetramer (*a* and *b*, *insets*), and the K_d was calculated from these latter plots by nonlinear analysis. The K_d was found to be 114 nmol during the primary response and 134 nmol during the memory response. In a second set of experiments, PBMC taken from donor NS 112 during the primary and memory response to EBV were stained with saturating concentrations of labeled tetramer on ice and then were washed and incubated with a 100-fold excess of unlabeled tetramer. Samples of the stained PBMC were analyzed before addition of unlabeled tetramer and then at 5, 10, 20, 40, 60, 90, and 120 min. The logarithm of the normalized total fluorescence was plotted against time to derive the dissociation curve (*c*). The curves from PBMC analyzed during the primary and memory responses were very similar.

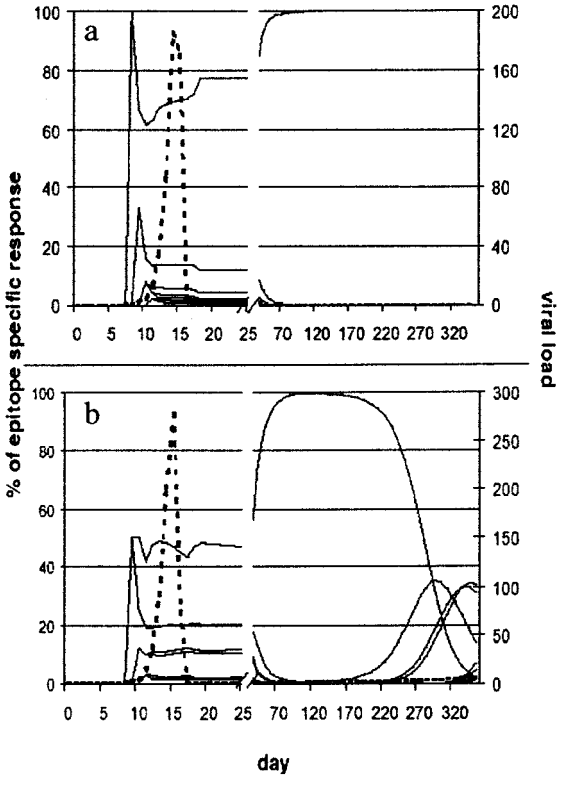

FIGURE 4. Comparison of T cell dominance in the basic model compared with the senescence model. The graphs track the contribution of individual T cells to the epitope-specific response over time. The percentage of contribution of individual clones is indicated by thin lines and shown on the *left axis*. The viral load is indicated by the thick broken line and is shown on the *right axis*. *a*, The output of the basic model, in which avidity is the only driving force for competition between T cell clones, predicts that a single high-avidity clone rapidly becomes dominant (competitive exclusion). *b*, The senescence model is characterized by contributions from several clones, the gradual senescence of high-avidity clones, and their slow replacement by clones of intermediate avidity (clonal succession).

in extensive down-regulation of these populations (Fig. 5*a*). The model predicts that T cells that were greatly expanded during the primary response will be preferentially down-regulated in the response at 1 year, and that smaller clones will be more likely to expand and replace them. We further analyzed the model output for the contribution of individual T cell clones to an epitope-specific response (Fig. 5*b*). Interestingly, the relationship between the $\log_2$ (cell number) of individual clones and the percentage of change is predicted to be complex and again closely resembles that found by experiment. Clones that expand dramatically during primary infection are more prone to die, whereas those that expand less dramatically may contribute relatively more to the response at 1 year. However, clones that are very poorly represented in the primary response are often actually further underrepresented at 1 year. This would appear at first to be counterintuitive and contrary

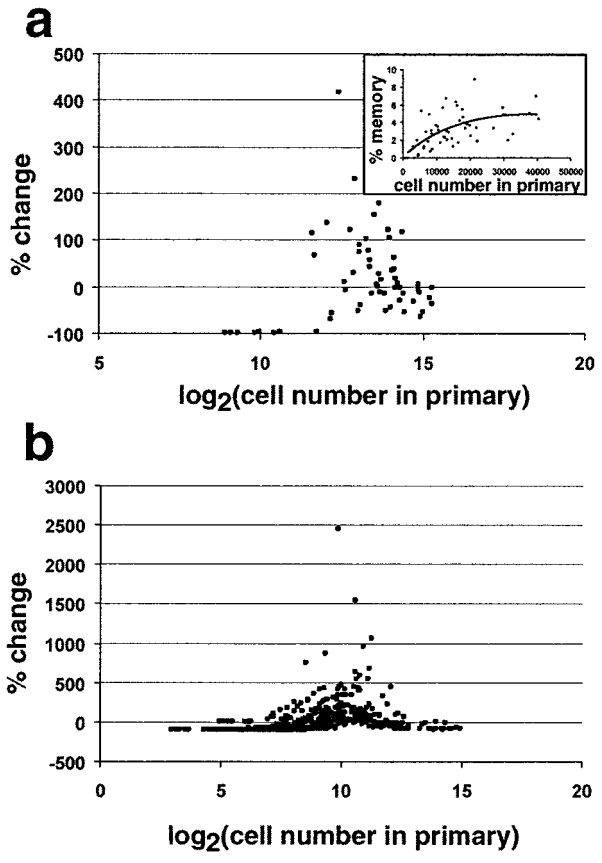

FIGURE 5. Relationship between cell divisions in the primary response and the down-regulation of the responses using the senescence model. The predicted relationship between the $\log_2$ of the number of epitope-specific T cells in the primary response vs the percentage of change in the frequency of the epitope-specific T cells between the primary response (at peak viral load) and the response at 300 days in the model. The number of epitope-specific T cells during the primary response is plotted against the percentage of these cells in the memory response at 1 year, derived from the model (*inset*). If the memory response were simply a fixed proportion of the primary response ($Y = MX$), then the relationship would be predicted to be a diagonal line. A relationship in which high cell division number in the primary response leads to a decreased contribution to the memory response ($Y = X(K - B \log_2(X))$, solid line) provides a better fit to the data ($R^2 = 0.47$; F test, $p < 0.0001$). *b*, The predicted relationship between the $\log_2$ of the number of epitope-specific T cells derived from a given clone and the percentage of change in frequency of epitope-specific T cells derived from that clone between the primary immune response and the response at 1 year. Parameters used for the simulation: $\pi = 2 \times 10^5$, $\delta = 0.2$, $X(0) = 1 \times 10^6$, $Y(0) = 1 \times 10^{-4}$, $\beta = 1 \times 10^{-10}$, $\mu = 10$, $\alpha = 0.01$, $k = 10$, $\lambda = \epsilon = \gamma = 1 \times 10^{-3}$, $r = 1$, $\omega = 0.1$, $C = 1.5$, $b_E = 0.5$, $\phi = 0.05$, $\theta = 1$, $p = 0.01$, $b_M = 0.01$, $\chi = 5 \times 10^{-3}$, $d_{sen} = 35$. Normal CD8 T cell numbers $= 5 \times 10^5$.

to the previous observations that the largest clones were most heavily down-regulated. However, the model predicts that at peak viremia, low avidity clones receive some stimulation and proliferate. During chronic infection, the lower levels of virus are insufficient to stimulate these clones, and thus they decline to very low levels. Therefore, the mathematical model provides an insight into why the experimental results suggest that both the largest and the smallest clones in the primary response will be relatively underrepresented in memory.

Discussion

A comparative analysis of the primary and memory $CD8^+$ T cell response to EBV revealed surprising differences between the responses. At the level of the epitopes recognized, we found that the most dominant epitopes became relatively less dominant over time. At the level of the T cell clonotypes responding to these epitopes, we found that those clonotypes that dominated the primary response were relatively less dominant 1 year later. Thus, the memory response was actually less focused than the primary response.

Our analysis was, inevitably, confined to the Ag-specific $CD8^+$ T cell populations within peripheral blood. Both primary and memory populations of T cells may traffic to different sites within the body and may be present at differing frequencies in spleen, lymph nodes, liver, bone marrow, and other tissues (29). Experiments performed in murine models of infection do show that the overall fall in numbers of Ag-specific T cells following the peak primary response may be less dramatic when all these other sites are also taken into account (29). Nevertheless, differences in patterns of recruitment seem unlikely to account for the differences in the extent of down-regulation of different populations of T cells that we have observed.

Changes in relative levels of expression of different viral proteins during the primary and persistent phases of infection may be one factor that influences shifts in immunodominance between primary and memory T cell responses. However, the observation that there are also changes in the clonal composition of the responses to individual epitopes suggests that other factors are likely to be involved in the evolution of T cell memory. In mouse models of primary and secondary responses, one such factor is ongoing affinity maturation (2–4, 6, 7). We have not found evidence for this in our study, and indeed we find that T cells have a relatively high avidity for the relevant tetrameric HLA-peptide complex at the time of first sampling during the primary response. The extent of exposure to Ag during primary EBV infection is likely to be high and more prolonged than during a single immunization, and hence the process of affinity maturation is likely to be advanced in our patients when they first donate blood. The differences observed between primary and memory responses must therefore reflect another biological process.

Statistical analysis revealed that it was the logarithm of the number of responding cells during the primary response that correlated with the extent of down-regulation of the response. Such a relationship provided a better fit to our data than a simple stochastic entry into memory model, in which the memory response would be linearly related to the primary response ($p = 0.0056$, Fig. 2*a*). An intuitive explanation for the findings was that T cells that have proliferated most extensively are more prone to die and are therefore less likely to be represented within the memory pool. We used computer models of T cell proliferation and death to test this idea formally. The initial model was adapted from conventional models of T cell proliferation and did not include the possibility of clonal senescence. Analysis of the numbers of cells responding to different epitopes in a simulated prime-boost scenario reproduced the enhanced immunodominance or epitope focusing seen in murine models of the response (2–4, 6, 7). However, analysis of the response at later time points in a simulated chronic infection showed a progressive focusing of the response. The model was then modified to incorporate the concept of cellular senescence. This required keeping track of cell division number in both the memory and effector compartment for each clone. The model was able to reproduce the observed effects of prime-boost in mice. However, the large Ag load and chronic Ag stimulation produced by simulation of EBV infection led to a different outcome from the previous model. The simple inclusion of a factor of cellular senescence in a model of affinity-driven clonal selection was sufficient

to reproduce the relationship observed in natural infection. Furthermore, in the presence of very high and sustained viral loads, this model predicts that all responding T cells may senesce (data not shown). This phenomenon of T cell exhaustion has been observed in the context of high dose lymphocytic choriomeningitis virus infection of mice (30–32).

We propose that the situation in natural EBV infection lies somewhere between the two extremes of acute low dose challenge (in which cells do not experience senescence phenomena because they do not undergo sufficient expansion) and immune exhaustion (in which responsiveness is lost due to senescence of all responding CTL) that have been reported in mouse models. Thus, EBV infection results in senescence and loss of some of the T cells that respond most vigorously in acute infection. However, T cells that have expanded less vigorously do not senesce and are able to maintain the response to virus. Because the term "exhaustion" has been associated with the failure of senescent CTL to be replaced (30–32), we prefer the term "clonal succession" to describe the sequential changes in dominance of the responding clones.

The mechanisms underlying senescence remain to be explored in more detail. They may involve an inability of the expanded populations of cells to modulate expression of survival factors (12, 33) or they may reflect other constraints such as telomere shortening.

Our experiments are performed in the setting of a natural infection in which Ag load is likely to be high during the primary phase of infection and very much lower during the persistent phase of infection. We are not able to perform experiments that address the question as to what would happen if further high dose challenge with Ag occurred in the context of EBV infection. Work on primary, memory, and secondary responses to influenza in mice has suggested that, while the frequency of the response that was immunodominant during primary infection fell to below that of a subdominant response in the resting memory phase, on secondary challenge the original hierarchy of immunodominance was reestablished (29).

It will, in the future, be interesting to analyze the response to different infections using similar methods to those described in this study and to ask whether cellular senescence might also constrain the response to other persistent virus infections such as HIV or to nonpersistent, but recurrent virus infections such as influenza. Certainly, any immune stimulus that can cause cells to undergo many rounds of cell division may be capable of causing immune senescence.

It is interesting to consider teleological arguments as to why T cell senescence may be beneficial to the host, despite the observed effect of the loss of high responder T cell clones. Cellular senescence is often thought of as a protection mechanism against neoplastic proliferation of cells. T cell senescence may also provide some protection from host death due to overwhelming infection and an excessive immune response or due to autoimmunity (32, 34). In this study, we suggest that cellular senescence within the cells of the immune system is an important adaptation that allows for a long-term effective T cell response to a persistent Ag. In the absence of senescence, modeling predicts that the T cell response to a pathogen would become progressively more focused, both at the level of the epitopes recognized and at the level of the clones responding to those epitopes. Ultimately, in the case of a persistent infection, the host response would depend on a single expanded clone recognizing a single epitope. Such a focused response renders the host extremely vulnerable to immunological escape by the pathogen. This study shows how T cell senescence prevents such extreme focusing and allows the immune response to remain relatively broad. A broad immune response comprising many different T cell clones recognizing several different epitopes renders the host less susceptible to virus escape mechanisms, and therefore represents a better biological response to a persistent infection.

Acknowledgments

We are grateful to Alan Perelson and Mark Davis for careful reading of the manuscript and to Mary Myerscough for helpful advice.

References

1. Maryanski, J. L., C. V. Jongeneel, P. Bucher, J. L. Casanova, and R. R. Walker. 1996. Single-cell PCR analysis of TCR repertoires selected by antigen in vivo: a high magnitude CD8 response is comprised of very few clones. *Immunity 4:47.*
2. McHeyzer-Williams, M. G., and M. M. Davis. 1995. Antigen-specific development of primary and memory T cells in vivo. *Science 268:106.*
3. Bachmann, M. F., D. E. Speiser, and P. S. Ohashi. 1997. Functional maturation of an antiviral cytotoxic T-cell response. *J. Virol. 71:5764.*
4. Busch, D. H., I. Pilip, and E. G. Pamer. 1998. Evolution of a complex T cell receptor repertoire during primary and recall bacterial infection. *J. Exp. Med. 188:61.*
5. Sourdive, D. J., K. Murali-Krishna, J. D. Altman, A. J. Zajac, J. K. Whitmire, C. Pannetier, P. Kourilsky, B. Evavold, A. Sette, and R. Ahmed. 1998. Conserved T cell receptor repertoire in primary and memory CD8 T cell responses to an acute viral infection. *J. Exp. Med. 188:71.*
6. Savage, P. A., J. J. Boniface, and M. M. Davis. 1999. A kinetic basis for T cell receptor repertoire selection during an immune response. *Immunity 10:485.*
7. Busch, D. H., and E. G. Pamer. 1999. T cell affinity maturation by selective expansion during infection. *J. Exp. Med. 189:701.*
8. Hou, S., L. Hyland, K. W. Ryan, A. Portner, and P. C. Doherty. 1994. Virus-specific CD8$^+$ T-cell memory determined by clonal burst size. *Nature 369:652.*
9. Callan, M. F. C., L. Tan, N. Annels, G. S. Ogg, J. D. Wilson, C. A. O'Callaghan, N. Steven, A. J. McMichael, and A. B. Rickinson. 1998. Direct visualization of antigen-specific CD8$^+$ T cells during the primary immune response to Epstein-Barr virus in vivo. *J. Exp. Med. 187:1395.*
10. Callan, M. F. C., N. Steven, J. Wilson, P. A. H. Moss, G. M. Gillespie, J. I. Bell, A. B. Rickinson, and A. J. McMichael. 1996. Large clonal expansions of CD8$^+$ T cells in acute infectious mononucleosis. *Nat. Med. 2:906.*
11. Tan, L. C., N. Gudgeon, N. E. Annels, P. Hansastua, C. O'Callaghan, S. Rowland-Jones, A. J. McMichael, A. B. Rickinson, and M. F. C. Callan. 1999. A re-evaluation of the frequency of CD8$^+$ T cells specific for EBV in healthy virus carriers. *J. Immunol. 162:1827.*
12. Callan, M. F. C., C. Fazou, H. B. Yang, T. Rostron, K. Poon, C. Hatton, and A. J. McMichael. 2000. CD8$^+$ T-cell selection, function, and death in the primary immune response in vivo. *J. Clin. Invest. 106:1251.*
13. Steven, N. M., A. M. Leese, N. E. Annels, S. P. Lee, and A. B. Rickinson. 1996. Epitope focusing in the primary cytotoxic T cell response to Epstein-Barr virus and its relationship to T cell memory. *J. Exp. Med. 184:1801.*
14. Globerson, A., and R. B. Effros. 2000. Ageing of lymphocytes and lymphocytes in the aged. *Immunol. Today 21:515.*
15. Nowak, M. A., and C. R. Bangham. 1996. Population dynamics of immune responses to persistent viruses. *Science 272:74.*
16. Nowak, M. A., R. M. May, R. E. Phillips, S. Rowland-Jones, D. G. Lalloo, S. McAdam, P. Klenerman, B. Koppe, K. Sigmund, C. R. Bangham, and A. J. McMichael. 1995. Antigenic oscillations and shifting immunodominance in HIV-1 infections. *Nature 375:606.*
17. Scotet, E., J. David-Ameline, M. A. Peyrat, A. Moreau-Aubry, D. Pinczon, A. Lim, J. Even, G. Semana, J. M. Berthelot, R. Breathnach, et al. 1996. T cell response to Epstein-Barr virus transactivators in chronic rheumatoid arthritis. *J. Exp. Med. 184:1791.*
18. Bogedain, C., H. Wolf, S. Modrow, G. Stuber, and W. Jilg. 1995. Specific cytotoxic T lymphocytes recognize the immediate-early transactivator Zta of Epstein-Barr virus. *J. Virol. 69:4872.*
19. Burrows, S. R., T. B. Sculley, I. S. Misko, C. Schmidt, and D. J. Moss. 1990. An Epstein-Barr virus-specific cytotoxic T cell epitope in EBNA 3A. *J. Exp. Med. 171:345.*
20. Sprent, J., and D. F. Tough. 2001. T cell death and memory. *Science 293:245.*
21. Murali-Krishna, K., J. D. Altman, M. Suresh, D. J. D. Sourdive, A. J. Zajac, J. D. Miller, J. Slansky, and R. Ahmed. 1998. Counting antigen-specific CD8 T cells: a reevalution of bystander activation during viral infection. *Immunity 8:177.*
22. Ogg, G. S., X. Jin, S. Bonhoeffer, P. Moss, M. A. Nowak, S. Monard, J. P. Segal, Y. Cao, S. L. Rowland-Jones, A. Hurley, et al. 1999. Decay kinetics of human immunodeficiency virus specific effector cytotoxic T lymphocytes after combination antiretroviral therapy. *J. Virol. 73:797.*
23. Van Stipdonk, M. J. B., E. E. Lemmens, and S. P. Schoenberger. 2001. Naive CTLs require a single brief period of antigenic stimulation for clonal expansion and differentiation. *Nat. Immun. 2:423.*
24. Kaech, S. M., and R. Ahmed. 2001. Memory CD8$^+$ T cell differentiation: initial antigen encounter triggers a developmental program in naive cells. *Nat. Immun. 2:415.*
25. Fasso, M., N. Anandasabapathy, F. Crawford, J. Kappler, C. G. Fathman, and

W. M. Ridgway. 2000. T cell receptor (TCR)-mediated repertoire selection and loss of TCR Vβ diversity during the initiation of a CD4$^+$ T cell response in vivo. *J. Exp. Med. 192:1719.*

26. Matsui, K., J. J. Boniface, P. Steffner, P. A. Reay, and M. M. Davis. 1995. Kinetics of T-cell receptor binding to peptide/I-Ek complexes: correlation of the dissociation rate with T-cell responsiveness. *Proc. Natl. Acad. Sci. USA 91:12862.*
27. Lyons, D. S., S. A. Lieberman, J. Hampl, J. J. Boniface, Y. Chien, L. J. Berg, and M. M. Davis. 1996. A TCR binds to antagonist ligands with lower affinities and faster dissociation rates than to agonists. *Immunity 5:53.*
28. Bousso, P., A. Casrouge, J. D. Altman, M. Hawy, J. Kanellopoulos, J. P. Abastado, and P. Kourilsky. 1998. Individual variations in the murine T cell response to a specific peptide reflect variability in naive repertoires. *Immunity 9:169.*
29. Marshall, D. R., S. J. Turner, G. T. Belz, S. Wingo, S. Andreansky, M. Y. Sangster, J. M. Riberdy, T. Liu, M. Tan, and P. C. Doherty. 2001. Measuring the diaspora for virus-specific CD8$^+$ T cells. *Proc. Natl. Acad. Sci. USA 98:6313.*
30. Moskophidis, D., F. Lechner, H. Pircher, and R. M. Zinkernagel. 1993. Virus persistence in acutely infected immunocompetent mice by exhaustion of antiviral cytotoxic effector T cells. *Nature 362:758.*
31. Gallimore, A., A. Glithero, A. Godkin, A. C. Tissot, A. Pluckthun, T. Elliott, H. Hengartner, and R. Zinkernagel. 1998. Induction and exhaustion of lymphocytic choriomeningitis virus-specific cytotoxic T lymphocytes visualized using soluble tetrameric major histocompatibility complex class I-peptide complexes. *J. Exp. Med. 187:1383.*
32. Oxenius, A., R. M. Zinkernagel, and H. Hengartner. 1998. Comparison of activation versus induction of unresponsiveness of virus-specific CD4$^+$ and CD8$^+$ T cells upon acute versus persistent viral infection. *Immunity 9:449.*
33. Grayson, J. M., A. J. Zajac, J. D. Altman, and R. Ahmed. 2000. Increased expression of Bcl-2 in antigen-specific memory CD8$^+$ T cells. *J. Immunol. 164: 3950.*
34. Anderton, S. M., C. G. Radu, P. A. Lowrey, E. S. Ward, and D. C. Wraith. 2001. Negative selection during the peripheral immune response to antigen. *J. Exp. Med. 193:1.*